Controls on ocean productivity and air-sea carbon flux: An adjoint model sensitivity study

S. Dutkiewicz, M. J. Follows, P. Heimbach, and J. Marshall

Department of Earth, Atmospheric and Planetary Sciences, Massachusetts Institute of Technology, Cambridge, Massachusetts, USA

Received 20 October 2005; revised 29 November 2005; accepted 7 December 2005; published 18 January 2006.

[1] We use the adjoint of a global model of coupled oceanic cycles of carbon, phosphorus and iron to comprehensively and efficiently map the sensitivity of global biological productivity and air-sea carbon fluxes to local perturbations of the atmospheric iron source sustained for a decade or more. Modeled productivity and carbon flux are found to be most sensitive to enhanced iron sources in high nitrate low chlorophyll regions. The relative response of productivity to an enhanced iron source is greatest in the Equatorial Pacific. Although surface macro-nutrients are more abundant in the Southern Ocean, nutrient utilization here is critically regulated by light limitation. Our results differ from those of previous studies which imposed depletion of surface nutrients and ignore the availability of light. However, the enhancement of oceanic carbon storage per unit increase in productivity is strongest in the high latitude oceans. **Citation:** Dutkiewicz, S., M. J. Follows, P. Heimbach, and J. Marshall (2006), Controls on ocean productivity and air-sea carbon flux: An adjoint model sensitivity study, *Geophys. Res. Lett.*, *33*, L02603, doi:10.1029/2005GL024987.

1. Introduction

[2] The first order global pattern of productivity is set by the wind-driven circulation, which regulates the availability of macro-nutrients and the interaction of surface ocean mixing and light. In some ocean upwelling regions, far from dust sources, this pattern is strongly modulated by the availability of iron [*Martin and Fitzwater*, 1988]. Field studies (reviewed by *de Baar et al.* [2005]) clearly demonstrate the enhancement of primary production by the addition of iron in these upwelling areas—the so-called high nitrate, low chlorophyll (HNLC) regions; the tropical Pacific, sub-Arctic Pacific and the Southern Ocean.

[3] Here we examine the large scale consequences of iron's control on productivity and carbon fluxes, on decadal to centennial time-scales, in a global model of the coupled oceanic iron, phosphorus and carbon cycles using the adjoint method. Adjoint approaches have previously been used for large scale biogeochemical optimizations [*Schlitzer*, 2002; *Matear and Holloway*, 1995]. This method allow us, here, to efficiently and comprehensively map the sensitivities of global productivity and carbon flux to perturbations in the iron source at any surface position. For context, we also examine the sensitivity to variations in incident photosynthetically active radiation (PAR).

0094-8276/06/2005GL024987$05.00

[4] Previous studies [e.g., *Sarmiento and Orr*, 1991; *Gnanadesikan et al.*, 2003; *Zeebe and Archer*, 2005] have also examined the sensitivity of atmospheric pCO_2 to regional iron "fertilization" on decadal to centennial time-scales. However, these studies did not comprehensively map local sensitivities (i.e., did not utilize the adjoint method) and did not explicitly represent the oceanic iron cycle. Instead they imposed changes in surface macro-nutrient concentrations ("nutrient depletion") or particle fluxes, assumed to represent local relief of iron stress. Here we explicitly represent the oceanic iron cycle following *Parekh et al.* [2005], representing scavenging, complexation and the aeolian source.

2. Forward Circulation and Biogeochemistry Model

[5] We overlay biogeochemical parameterizations on the MIT ocean circulation model [*Marshall et al.* 1997] configured globally at coarse resolution (2.8 × 2.8 degrees, 15 vertical levels [see *Dutkiewicz et al.*, 2005]). Prognostic tracers are inorganic and organic forms of phosphorus, carbon, iron, along with alkalinity. We apply a simplified parameterization of net community production, B, which is regulated by the availability of PAR (I), phosphate (PO_4), and iron (Fe):

$$B(x,y,z) = \alpha \frac{I(x,y,z)}{I(x,y,z)+K_I} \cdot \frac{PO_4(x,y,z)}{PO_4(x,y,z)+K_{PO_4}} \cdot \frac{Fe(x,y,z)}{Fe(x,y,z)+K_{Fe}} \quad (1)$$

where $\alpha = 6\ \mu\text{M P y}^{-1}$, and the half saturation constants are $K_I = 20\ \text{W m}^{-2}$, $K_{PO_4} = 0.5\ \mu\text{M}$ and $K_{Fe} = 0.12\ \text{nM}$. Two thirds of the organic matter produced enter the dissolved organic pool and are assumed to have an e-folding remineralization timescale of 6 months. The remaining fraction is instantaneously exported to depth as particulate matter and remineralized according to *Martin et al.* [1987]. Biological transformations to and from organic form are assumed to occur in fixed elemental ratios. We represent the scavenging and complexation of iron following *Parekh et al.* [2005] with an aeolian source prescribed from the model of *Mahowald et al.* [2003]. Two per-cent of dust-borne iron enters the dissolved pool, within the range suggested by *Jickells and Spokes* [2001]. The air-sea exchange of CO_2 is parameterized following *Wanninkhof* [1992].

[6] After several thousand years of spin up with a fixed atmospheric pCO_2 of 278 ppmv, the model reaches a steady state. The model reproduces the general character of

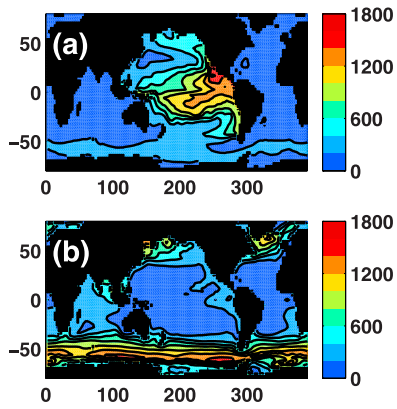

Figure 1. Adjoint derived response of globally averaged net community production to decade-long perturbations of aeolian iron source and PAR: $\frac{1}{A(x,y)}(\frac{\partial J_B}{\partial X}\Delta X)$ where $A(x, y)$ is the area of the grid cell over which the perturbation is applied and ΔX is the magnitude of the imposed perturbation. Results are expressed in carbon units assuming fixed, Redfieldian, C:P stoichiometry. (Units: g C m^{-2}; contour interval: 200 g Cm^{-2}). (a) Response to perturbed aeolian iron source: $X = F_{Fe}(x, y)$, $\Delta X = +0.02$ mmol m^{-2} y^{-1} bio-available Fe. (b) Response to perturbed photosynthetically active radiation: $X = I(x, y)$, $\Delta X = +30$ W m^{-2}. The figures map the changes in global productivity over a 10 year period in response to a continuous perturbation, ΔX, at each model surface grid cell.

observed gradients of PO_4 both in the surface and deep ocean and has elevated surface PO_4 concentrations in HNLC regions. Notably, though, surface PO_4 in the equatorial Pacific in this configuration is higher than observed, related to the issue of nutrient trapping [*Najjar et al.*, 1992] and due to the coarse resolution [*Aumont et al.*, 1999]. Though observations remain sparse, modeled surface iron concentrations are plausibly elevated in the surface waters of the Atlantic and Indian Oceans which receive the strongest dust flux, and low in equatorial Pacific and Southern Oceans [see *Parekh et al.*, 2005].

3. Sensitivity Analysis

[7] We use the adjoint of the model to evaluate the sensitivities of productivity (defined by equation (1)) and air-sea carbon fluxes to decadal scale variations in the surface source of iron and insolation. The adjoint was developed using the automatic differentiation (AD) tool, TAF (Transformation of Algorithms in Fortran) [*Giering and Kaminski*, 1998; *Heimbach et al.*, 2005]. This approach has been applied to sensitivity studies and state estimation of ocean circulation [e.g., *Marotzke et al.*, 1999; *Stammer et al.*, 2004] and an idealized tracer sensitivity study [*Hill et al.*, 2004]. Here, we describe its first application to explicit biogeochemical cycles. In this method, an objective ("cost") function, J, is defined; this is a measure of the model state which can be evaluated through a forward integration. Subsequently a "backward" integration of the adjoint model returns the gradient, or sensitivity, of the cost function, $\frac{\partial J}{\partial X}$, with respect to a set of control variables, X (see *Marotzke et al.* [1999] for more details).

3.1. Global Community Production

[8] Here we define the cost function as the integral of global community production (equation (1)) over a given time interval, Δt:

$$J_B = \int_t^{t+\Delta t} \int B(x,y,z)\ dV\ dt\ . \qquad (2)$$

The adjoint apparatus determines the partial derivative at each surface grid cell of the ocean model evaluated around a time-evolving (but unperturbed model trajectory), $\frac{\partial J_B}{\partial X}$, where X is either the flux of iron dust, $F_{Fe}(x, y)$, or PAR, $I(x, y)$. The sensitivity map thus obtained is equivalent to performing many decadal perturbation experiments in which the additional external source of iron or light is applied continuously to each surface grid cell, one by one, and the response in global productivity individually evaluated. Such individual experiments would have a computational cost several orders of magnitude greater than the adjoint approach used here. Comparisons indicate that the adjoint method returns the sensitivities determined by individual perturbation experiments with an accuracy of the order of one percent [see also *Hill et al.*, 2004].

[9] We illustrate the sensitivity of productivity in response to ten years of continuous, additional aeolian iron source (Figure 1a): $\frac{1}{A(x,y)}(\frac{\partial J_B}{\partial X}\Delta X)$ where ΔX = 0.02 mmol m^{-2} y^{-1} of bio-available iron. The unperturbed aeolian iron source provided to the model exhibits strong regional variations, ranging from less than 0.001 mmol m^{-2} y^{-1} bio-available iron over the Southern Ocean and Equatorial Pacific to greater than 0.5 mmol m^{-2} y^{-1} over subtropical Atlantic and Northern Indian. A 0.02 mmol m^{-2} y^{-1} perturbation might result from long term changes in patterns of dust deposition due to variations in climate, atmospheric washout, changes in land use, or deliberate anthropogenic iron addition. In some regions of low aeolian deposition (e.g., the Southern Ocean) the imposed perturbation is significant; though possibly the magnitude of glacial/interglacial change. The local values on the map (Figure 1a) indicate the change in global biological productivity caused by the perturbation at that grid cell during the 10 years. Higher values indicate a more intense response of global productivity to the additional iron supplied at that grid cell. This response not only includes direct local changes to productivity, but also non-local effects, such as "downstream" fertilization due to the transport of excess iron from the perturbed source.

[10] Over most of the ocean an additional iron source leads to an increase in global productivity on this timescale. The Atlantic is insensitive to the increase in iron since the perturbation is small relative to the dust source in this region and, moreover, the Atlantic is significantly limited by the supply of macro-nutrients [e.g., *Mills et al.*, 2004; *Dutkiewicz et al.*, 2005]. We note, though, that the model does not represent the cycling of nitrogen, and therefore the potential of additional iron to increase nitrogen fixation; a process that may be important in the North Atlantic subtropics. Consistent with field experiments [e.g., *de Baar et al.*, 2005; *Buesseler et al.*, 2005] global productivity is

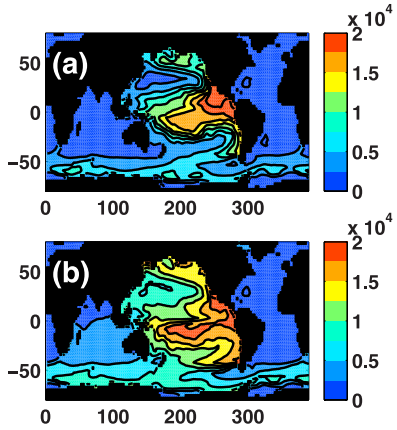

Figure 2. Adjoint derived sensitivity of model global CO_2 flux to a continuous additional source of bio-available iron: $\frac{1}{\Delta X \cdot A(x,y) \cdot \Delta t}(\frac{\partial J_{F_{CO2}}}{\partial X}\Delta X)$, where X is the aeolian iron flux, and $\Delta X = 0.02$ mmol m^{-2} y^{-1} bio-available Fe. (Units: ton C/ton Fe; contour interval: 2500 ton C/ton Fe.) (a) after 10 years; (b) after 100 years. The figures map the global mass of carbon sequestered in to the ocean over the perturbation period per ton of additional bio-available iron supplied at each model surface grid cell.

particularly sensitive to additional iron sources in the HNLC regions.

[11] The model suggests that the strongest response in global productivity over ten years occurs in the equatorial Pacific. We might expect a more significant impact in the Southern Ocean where there are much higher concentrations of unutilized surface macro-nutrients. However, over the course of the annual cycle, other factors are important in limiting Southern Ocean productivity. During winter months at higher latitudes, very low insolation and deep mixed layers shut down primary production. Additional iron sources during those months will be not be utilized and are partially lost to scavenging. During the relatively short growing season, the enhancement of the iron source in the Southern Ocean does increase productivity in the model (Figure 1a). However, even during the growing season, relatively deep mixed-layers can cause some light limitation, or co-limitation, reducing the role of iron as a limiting nutrient [*de Baar et al.*, 2005; *van Oijen et al.*, 2004; *Sunda and Huntsman*, 1997; *Hiscock et al.*, 2003].

[12] We illustrate the importance of light control by mapping the corresponding sensitivity of global productivity to a highly idealized, year-round perturbation in surface incident PAR (Figure 1b): $\frac{1}{A(x,y)}(\frac{\partial J_B}{\partial X}\Delta X)$ where $\Delta X =$ 30W m^{-2}. The strong response to increased PAR at high Southern latitudes reinforces the important control of light in that region of the model. In contrast, in the equatorial Pacific, which in our model has the lowest surface iron concentrations, light is not limiting (Figure 1b), hence iron added at any time of year can be utilized.

[13] We note that the quantitative details of the model sensitivities are dependent upon the simplifications and coarse resolution of the underlying model. Thus the high sensitivity in the Equatorial Pacific may be partly due to overestimated macro-nutrient concentrations present in the forward integration, largely a consequence, we believe, of coarse resolution.

3.2. Global Air-Sea Flux of CO_2

[14] Defining a new cost function we may also evaluate the sensitivity of the net global air-sea flux of CO_2 (F_{CO2}) over the time period in which the perturbation in the iron source is applied:

$$J_{F_{CO2}} = \int_t^{t+\Delta t} \int F_{CO2}(x,y)\ dA\ dt. \tag{3}$$

We examine the response to a perturbation sustained over ten years (Figure 2a) and one hundred years (Figure 2b), scaled to illustrate the sensitivity in terms of tons of carbon sequestered in the ocean per additional ton of bio-available iron added. Atmospheric pCO_2 is assumed to be constant here since the drawdown of atmospheric CO_2 from any single perturbation experiment is negligible. Naturally, the sensitivity of global ocean carbon uptake after ten years of perturbation closely reflects that of global productivity (Figure 1a) with sensitivities higher in the HNLC regions and highest in the Equatorial Pacific. The pattern does change as the timescale of the perturbation is increased. After 100 years of perturbed fluxes (Figure 2b) there are additional downstream impacts. For instance, additional iron sources in the Indian Ocean of our model have little impact on global carbon uptake over 10 years but impacts productivity and CO_2 fluxes more significantly after 100 years by providing a remote source to regions of the Southern Ocean and Equatorial Pacific. Moreover some regions of the eastern Equatorial Pacific have less impact on global carbon uptake after 100 years when macro-nutrients have been stripped out of the surface waters.

[15] Mapping the relative sensitivities of productivity and air-sea carbon flux, $(\frac{\partial J_{F_{CO_2}}}{\partial X}\Delta X)/(\frac{\partial J_B}{\partial X}\Delta X)$, where X is the aeolian iron flux (not shown) reveals that globally, in our model, only ~20% of the enhanced community production translates into increased ocean carbon uptake. In part, this reflects the fact that most of the organic matter produced remineralizes to an inorganic form in the surface waters on a timescale shorter than that for air-sea equilibration. The productivity stimulated by the perturbation to the iron source is most efficiently translated into an oceanic uptake of carbon in the subpolar oceans (~25%), including the Southern Ocean, where the dissolved organic fraction is more rapidly mixed away from the surface. The least efficient regions are the subtropical gyres (~15%).

4. Discussion and Summary

[16] We have used the adjoint method to elucidate the sensitivity of biological productivity and air-sea carbon flux to perturbations in the surface sources of iron and PAR in a global model. Although our study is somewhat idealized, sensitivities on decadal to centennial timescales are relevant to those that result from natural shifts in climatic regimes or, in the case of iron, discussions of deliberate fertilization. The adjoint method provides a comprehensive and efficient evaluation of model sensitivities which we have exploited here to provide a clear view of the relative regional sensitivities in the model; the equivalent of many thousands

of individual perturbation studies at a fraction of the computational expense.

[17] Our study highlights the constraints on productivity due to the explicit interactions of iron and phosphorus cycles and light limitation. These interactions limit the ability to enhance export and reduce surface macro-nutrient concentrations in the Southern Ocean, processes which are not captured in "nutrient-depletion" studies [e.g., *Sarmiento and Orr*, 1991] in which macro-nutrients can be drawn down to arbitrary low levels. Although the Southern Ocean is iron stressed in our model we find that light limitation also plays a major controlling role in regulating large scale patterns of nutrient utilization, annual productivity and air-sea carbon fluxes. In consequence our study significantly reduces the relative efficiency of iron fertilization in the Southern Ocean and emphasizes the sensitivity of the tropical Pacific Ocean. However, high latitudes, including the Southern Ocean, are more efficient in sequestering carbon from enhanced biological production.

[18] This study illustrates the power of the adjoint sensitivity method and indicates some interesting consequences of the interplay of phosphorus, iron and light limitation in the framework of this model. The maps of sensitivity are revealing but, due to the idealized nature of the studies, the coarse resolution of the model, the lack of explicit ecosystem dynamics, and ignoring the impacts of iron on nitrogen fixation, should be regarded as preliminary, qualitative representations. They provide a context for further studies with more detailed, higher resolution models.

[19] Finally, with regard to discussions of deliberate iron fertilization of the oceans, we note that in the same model framework, studies of a globally averaged, five-fold increase in the aeolian iron source for a thousand years, suggest a global draw-down of atmospheric pCO_2 on the order of 10ppmv [*Parekh et al.*, 2006], in common with models of *Archer et al.* [2000] and *Bopp et al.* [2003]. Relative to a present day anthropogenic increase on the order of 1ppmv per year this does not suggest fertilization as a viable mitigation strategy, supporting the findings of *Zeebe and Archer* [2005].

[20] **Acknowledgments.** We thank Ralf Giering of FastOpt for assistance with TAF, and two anonymous reviewers for constructive comments. We are grateful for the following support: M. J. F. and S. D. from NOAA (NA16GP2988); M. J. F. from NSF (OCE-336839); J. M. from DOE; P. H. from NOPP (NSF, NASA, NOAA) and the NSF ITR program (ACI 0121182).

References

Archer, D., A. Winguth, D. Lea, and N. Mahowald (2000), What caused the glacial/interglacial atmospheric pCO_2 cycles?, *Rev. Geophys.*, *38*, 159–189.

Aumont, O., J. Orr, P. Monfray, G. Madec, and E. Maier-Reimer (1999), Nutrient trapping in the equatorial Pacific: The ocean circulation solution, *Global Biogeochem. Cycles*, *13*, 351–369.

Bopp, L., K. Kohfeld, and C. Le Qur (2003), Dust impact on marine biota and atmospheric CO_2, *Paleoceanography*, *18*(2), 1046, doi:10.1029/2002PA000810.

Buesseler, K. O., J. E. Andrews, S. Pike, M. A. Charette, L. E. Goldson, M. A. Brzezinski, and V. P. Lance (2005), Particle export during the Southern Ocean Iron Experiment (SOFeX), *Limnol. Oceanogr.*, *50*, 311–327.

de Baar, H. J. W., et al. (2005), Synthesis of iron fertilization experiments: From the iron age in the age of enlightenment, *J. Geophys. Res.*, *110*, C09S16, doi:10.1029/2004JC002601.

Dutkiewicz, S., M. Follows, and P. Parekh (2005), Interactions of the iron and phosphorus cycles: A three-dimensional model study, *Global Biogeochem. Cycles*, *19*, GB1021, doi:10.1029/2004GB002342.

Giering, R., and T. Kaminski (1998), Recipes for adjoint code construction, *Trans. Math. Software*, *24*, 437–474.

Gnanadesikan, A., J. L. Sarmiento, and R. D. Slater (2003), Effects of patchy ocean fertilization on atmospheric carbon dioxide and biological production, *Global Biogeochem. Cycles*, *17*(2), 1050, doi:10.1029/2002GB001940.

Heimbach, P., C. N. Hill, and R. Giering (2005), An efficient exact adjoint of the parallel MIT general circulation model, generated via automatic differentiation, *Future Gener. Comput. Syst.*, *21*, 1356–1371, doi:10.1016/j.future.2004.11.010.

Hill, C. N., V. Bugion, M. J. Follows, and J. C. Marshall (2004), Evaluating carbon sequestration efficiency in an ocean model using adjoint sensitivity analysis, *J. Geophys. Res.*, *109*, C11005, doi:10.1029/2002JC001598.

Hiscock, M. R., J. Marra, W. O. Smith Jr., R. Goericke, C. I. Measures, S. Vink, R. J. Olson, H. M. Sosik, and R. T. Barber (2003), Primary productivity and its regulation in the Pacific sector of the Southern Ocean, *Deep Sea Res., Part II*, *50*, 533–558.

Jickells, T. D., and L. J. Spokes (2001), Atmospheric iron inputs to the oceans, in *The Biogeochemistry of Iron in Seawater*, edited by D. R. Turner and K. A. Hunter, pp. 85–121, John Wiley, Hoboken, N. J.

Mahowald, N., C. Lou, J. del Corral, and C. Zender (2003), Interannual variability in atmospheric mineral aerosols from a 22-year model simulation and observational data, *J. Geophys. Res.*, *108*(D12), 4352, doi:10.1029/2002JD002821.

Marotzke, J., R. Giering, K. Q. Zhang, D. Stammer, C. Hill, and T. Lee (1999), Construction of the adjoint MOT ocean general circulation model and application to Atlantic heat transport sensitivity, *J. Geophys. Res.*, *104*, 29,529–29,547.

Marshall, J. C., C. Hill, L. Perelman, and A. Adcroft (1997), Hydrostatic, quasi-hydrostatic and non-hydrostatic ocean modeling, *J. Geophys. Res.*, *102*, 5733–5752.

Martin, J. H., and S. Fitzwater (1988), Iron deficiency limits phytoplankton growth in the north-east Pacific subarctic, *Nature*, *331*, 341–343.

Martin, J., G. Knauer, D. Karl, and W. Broenkow (1987), VERTEX: Carbon cycling in the northeast Pacific, *Deep Sea Res.*, *34*, 267–285.

Matear, R., and G. Holloway (1995), Modeling the inorganic phosphorus cycle of the North Pacific using an adjoint data assimilation model to assess the role of dissolved organic phosphorus, *Global Biogeochem. Cycles*, *9*, 101–119.

Mills, M., C. Ridame, M. Davey, J. L. Roche, and R. Geider (2004), Iron and phosphorus co-limit nitrogen fixation in the eastern tropical North Atlantic, *Nature*, *429*, 292–294.

Najjar, R. G., J. L. Sarmiento, and J. R. Toggweiler (1992), Downward transport and fate of organic matter in the ocean: Simulations with a general circulation model, *Global Biogeochem. Cycles*, *6*, 403–462.

Parekh, P., et al. (2006), Atmospheric carbon dioxide in a less dusty world, *Geophys. Res. Lett.*, doi:10.1029/2005GL025098, in press.

Parekh, P., M. J. Follows, and E. A. Boyle (2005), Decoupling of iron and phosphate in the global ocean, *Global Biogeochem. Cycles*, *19*, GB2020, doi:10.1029/2004GB002280.

Sarmiento, J. L., and J. C. Orr (1991), Three-dimensional simulation of the impact of southern ocean nutrient depletion on atmospheric CO_2 and ocean chemistry, *Limnol. Oceanogr.*, *36*, 1928–1950.

Schlitzer, R. (2002), Carbon export fluxes in the Southern Ocean: Results from inverse modeling and comparison with satellite based estimates, *Deep Sea Res., Part II*, *49*, 1623–1644.

Stammer, D., K. Ueyoshi, A. Köhl, W. B. Large, S. Josey, and C. Wunsch (2004), Estimating air-sea flux estimates through global ocean data assimilation, *J. Geophys. Res.*, *109*, C05023, doi:10.1029/2003JC002082.

Sunda, W. G., and S. A. Huntsman (1997), Interrelated influence of iron, light and cell size on marine phytoplankton growth, *Nature*, *390*, 389–392.

van Oijen, T., M. A. van Leeuwe, E. Granum, F. J. Weissing, R. G. J. Bellerby, W. W. C. Gieskes, and H. J. W. de Baar (2004), Light rather than iron controls photosythate production and allocation in Southern Ocean phytoplankton populations during austral autumn, *J. Plankton Res.*, *26*, 885–900.

Wanninkhof, R. (1992), Relationship between wind speed and gas exchange over the ocean, *J. Geophys. Res.*, *97*, 7373–7382.

Zeebe, R. E., and D. Archer (2005), Feasibility of ocean fertilization and its impacts on future atmospheric CO_2 levels, *Geophys. Res. Lett.*, *32*, L09703, doi:10.1029/2005GL022449.

S. Dutkiewicz, M. J. Follows, P. Heimbach, and J. Marshall, Department of Earth, Atmospheric and Planetary Sciences, Massachusetts Institute of Technology, 54-1412, 77 Massachusetts Avenue, Cambridge, MA 02139, USA. (stephd@ocean.mit.edu)